



## Evolution of local work function in epitaxial VO<sub>2</sub> thin films spanning the metal-insulator transition

Ahrum Sohn, Haeri Kim, Dong-Wook Kim, Changhyun Ko, Shriram Ramanathan, Jonghyurk Park, Giwan Seo, Bong-Jun Kim, Jun-Hwan Shin, and Hyun-Tak Kim

Citation: *Applied Physics Letters* **101**, 191605 (2012); doi: 10.1063/1.4766292

View online: <http://dx.doi.org/10.1063/1.4766292>

View Table of Contents: <http://scitation.aip.org/content/aip/journal/apl/101/19?ver=pdfcov>

Published by the [AIP Publishing](#)

---

### Articles you may be interested in

[Light scattering by epitaxial VO<sub>2</sub> films near the metal-insulator transition point](#)

*J. Appl. Phys.* **117**, 184304 (2015); 10.1063/1.4921057

[Optimization of the semiconductor-metal transition in VO<sub>2</sub> epitaxial thin films as a function of oxygen growth pressure](#)

*Appl. Phys. Lett.* **104**, 081913 (2014); 10.1063/1.4866806

[Comprehensive study of the metal-insulator transition in pulsed laser deposited epitaxial VO<sub>2</sub> thin films](#)

*J. Appl. Phys.* **113**, 043707 (2013); 10.1063/1.4788804

[Increased metal-insulator transition temperatures in epitaxial thin films of V<sub>2</sub>O<sub>3</sub> prepared in reduced oxygen environments](#)

*Appl. Phys. Lett.* **98**, 152105 (2011); 10.1063/1.3574910

[Metal-insulator transition in epitaxial V<sub>1-x</sub>W<sub>x</sub>O<sub>2</sub> \(0 ≤ x ≤ 0.33\) thin films](#)

*Appl. Phys. Lett.* **96**, 022102 (2010); 10.1063/1.3291053

---

An advertisement for Applied Physics Reviews Special Topic Sections. The background is a dark blue gradient with a bright light source on the right, creating a lens flare effect. On the left, there is a small image of a book cover for 'AIP Applied Physics Reviews' featuring a diagram of a layered structure. The main text 'NEW Special Topic Sections' is in large, white, bold font. Below it, 'NOW ONLINE' is in yellow, followed by 'Lithium Niobate Properties and Applications: Reviews of Emerging Trends' in white. The AIP Applied Physics Reviews logo is in the bottom right corner.

**NEW Special Topic Sections**

**NOW ONLINE**  
Lithium Niobate Properties and Applications:  
Reviews of Emerging Trends

**AIP** Applied Physics  
Reviews

## Evolution of local work function in epitaxial VO<sub>2</sub> thin films spanning the metal-insulator transition

Ahrum Sohn,<sup>1</sup> Haeri Kim,<sup>1</sup> Dong-Wook Kim,<sup>1,2,a)</sup> Changhyun Ko,<sup>3</sup> Shriram Ramanathan,<sup>3</sup> Jonghyurk Park,<sup>4</sup> Giwan Seo,<sup>5,6</sup> Bong-Jun Kim,<sup>5</sup> Jun-Hwan Shin,<sup>5,6</sup> and Hyun-Tak Kim<sup>5,6,b)</sup>

<sup>1</sup>Department of Physics, Ewha Womans University, Seoul 120-750, South Korea

<sup>2</sup>Department of Chemistry and Nano Science, Ewha Womans University, Seoul 120-750, South Korea

<sup>3</sup>School of Engineering and Applied Sciences, Harvard University, Cambridge, Massachusetts 02138, USA

<sup>4</sup>Electronics and Telecommunications Research Institute (ETRI), Daejeon 305-350, South Korea

<sup>5</sup>Metal-Insulator Transition Laboratory, ETRI, Daejeon 305-350, South Korea

<sup>6</sup>School of Advanced Device Technology, University of Science and Technology, Daejeon 305-333, South Korea

(Received 30 August 2012; accepted 23 October 2012; published online 8 November 2012)

Transport and Kelvin probe force microscopy measurements were simultaneously conducted on epitaxial VO<sub>2</sub> thin films. The sample's work function abruptly dropped from 4.88 eV to 4.70 eV during heating from 333 K to 353 K, suggesting a significant change in its electronic band structure spanning the metal insulator transition. The work function showed nearly no statistical deviation across the film's surface during the transition, likely due to band bending at the boundaries of the small domains. Resistance profiles confirmed that the local work function corresponded closely to the resistance of the corresponding area. © 2012 American Institute of Physics. [<http://dx.doi.org/10.1063/1.4766292>]

VO<sub>2</sub>, a representative correlated electron system, shows a metal-insulator transition (MIT) and a tetragonal-monoclinic structural phase transition (SPT) at around 340 K.<sup>1–12</sup> The MIT induces significant changes in electrical and optical properties, which could be used in various devices. During the transitions, two distinct electronic and/or structural phases coexist and various experiments with micro- and nano-scopic spatial resolution have been attempted to unveil the mechanism.<sup>4–10</sup> The nanoscale dichotomy of the MIT and the SPT—the decoupling of the electronic and structural changes—in VO<sub>2</sub> thin films has been observed.<sup>10</sup> SPT hysteresis in polycrystalline VO<sub>2</sub> thin films has also been reported to be wider than that induced by MIT.<sup>11</sup> Further nanoscopic characterization of VO<sub>2</sub>'s electronic properties are required to achieve better understanding of its MIT.

Kelvin probe force microscopy (KPFM) can assess the local work function of a sample ( $W_{\text{sample}}$ ), which is determined by its band structure.<sup>8,14</sup> Maps of  $W_{\text{sample}}$  can be used to examine spatial band bending in granular semiconductor thin films.<sup>14</sup> This work reports KPFM observations of the abrupt decrease of VO<sub>2</sub> thin films' local work function during heating above the material's MIT temperature ( $T_{\text{MIT}}$ ). Statistical deviation of the local  $W_{\text{sample}}$  showed little dependence on temperature during the MIT, contrary to the expectation that coexisting metallic and semiconducting phases might lead to variations of local work function across the thin film. Local work function in the small semiconducting domains could be reduced due to band bending by neighboring metallic domains. Modification of carrier concentration should influence the phase transition behavior of the VO<sub>2</sub> thin films.

Thin films of VO<sub>2</sub> were deposited on Al<sub>2</sub>O<sub>3</sub> (0001) substrates at 550 °C by reactive RF magnetron sputtering. The epitaxial films' multiple domains were confirmed by x-ray

diffraction (XRD) and transmission electron microscopy measurements. Samples' detailed characteristics are reported elsewhere.<sup>3,10</sup> Planar junctions with 4 μm wide and 4 μm gapped Au/Ti electrodes were prepared by conventional photolithography and lift off. Transport characteristics were investigated under an external bias voltage ( $V_{\text{ext}}$ ) applied to the electrodes using a Hewlett-Packard 4156B semiconductor parameter analyzer.

KPFM measurements were conducted using a scanning probe microscopy system (XE-100, Park Systems Co., Korea). Pt-coated Si cantilevers (NSC10/Pt, Micromasch, Estonia) were used in non-contact mode. Sample temperature was controlled by a heating stage. The tip's work function was calibrated using a highly oriented pyrolytic graphite reference. Topography was measured in AC mode with a drive frequency of 222 kHz (slightly lower than the resonance frequency of the cantilever). Surface potential measurements were simultaneously acquired by applying an AC modulation voltage of amplitude ( $V_{\text{ac}}$ ) 2 V and frequency 20 kHz to the tip. Figure 1 shows a schematic diagram of the transport and KPFM measurements of the VO<sub>2</sub> film.

Spatial maps of  $W_{\text{sample}}$  were obtained at three different temperatures, as shown in Figure 2(a). Average local work function over 1 μm<sup>2</sup> abruptly dropped from 4.88 to 4.70 eV at 348 K, suggesting a significant change in the electronic structure [Fig. 2(b)]. VO<sub>2</sub> has a 3d<sup>1</sup> electron system and splitting of the lowest-energy  $t_{2g}$  states is known to open a gap at low temperatures.<sup>2,3</sup> The material's resistance also sharply decreased at similar temperatures (Fig. 2(b), note the log-scale resistance axis). Based on a percolation model, the resistance of the electronically inhomogeneous system should be explained by the connectivity of metallic domains.<sup>6</sup>

The films were heated at 373 K for 30 min immediately prior to the KPFM measurements to remove possible water adsorbates.<sup>15</sup> The films were then cooled to ~330 K and the KPFM measurements were performed during heating to

<sup>a)</sup>E-mail: dwkim@ewha.ac.kr.

<sup>b)</sup>E-mail: htkim@etri.re.kr.

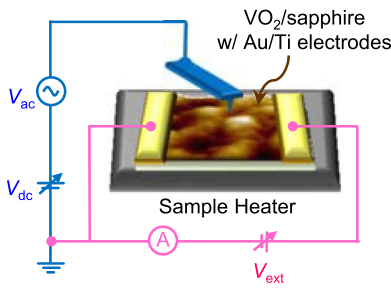


FIG. 1. The VO<sub>2</sub> film and the experimental configurations for transport and KPFM measurements.

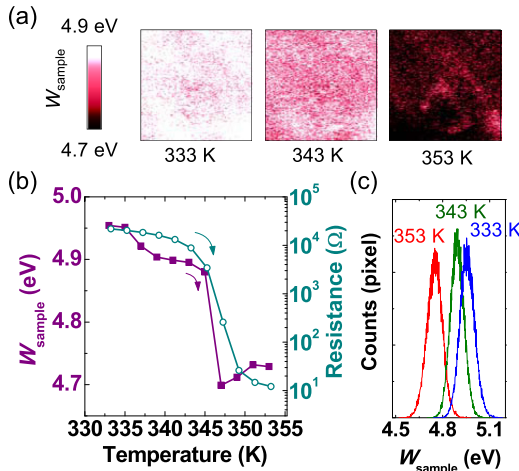


FIG. 2. (a)  $W_{\text{sample}}$  maps obtained at three temperatures during the heating (upper row) and cooling (lower row) of a VO<sub>2</sub> thin film (area 1  $\mu\text{m}^2$ ), (b)  $W_{\text{sample}}$  and resistance curves with respect to temperature, and (c) histograms of  $W_{\text{sample}}$  maps at three temperatures during heating.

$\sim 360$  K. The sharp drop of  $W_{\text{sample}}$  could only be observed after such prior heat treatment, otherwise the samples showed a gradual and slight decrease of  $W_{\text{sample}}$  ( $\sim 0.05$  eV) as the observation temperature increased to 360 K. The samples' surfaces, exposed to the ambient atmosphere, allowed the adsorption of water, resulting in surface dipoles that hindered observation of the material's inherent  $W_{\text{sample}}$ .<sup>15,16</sup> Recent KPFM observation of vanadium oxide has also shown that near-surface composition can alter the work function change during the transition.<sup>8</sup>

Ultraviolet photoelectron spectroscopy has shown a decrease of  $W_{\text{sample}}$  from 4.10 eV to 3.65 eV.<sup>13</sup> This change, 0.45 eV, is much larger than the 0.18 eV observed here by KPFM, despite both methods observing a reduction of  $W_{\text{sample}}$  during the MIT. This may be in part due to differences in the measurement conditions: the previous work measured minimum  $W_{\text{sample}}$  values using single crystalline nanorods under ultrahigh vacuum; this work recorded average  $W_{\text{sample}}$  values of epitaxial thin films in air.<sup>16</sup>

XRD peaks of VO<sub>2</sub> thin film have been shown to widen near the transition temperature,<sup>6,10</sup> due to the superposition of two distinct structural phases coexisting during the structural transition. In such an inhomogeneous system, a simple relation for the averaged  $W_{\text{sample}}$  can be suggested

$$W_{\text{sample}}(T) = W_{\text{sample,M}} \times [1 - f(T)] + W_{\text{sample,S}} \times f(T), \quad (1)$$

where  $f$  is the fraction of semiconducting domains, and  $W_{\text{sample,M}}$  and  $W_{\text{sample,S}}$ , respectively, indicate the work functions of the metallic and semiconducting domains. In the case of VO<sub>2</sub> single crystals,  $W_{\text{sample,M}}$  and  $W_{\text{sample,S}}$  have little dependence of on temperature.<sup>4,5</sup> Assuming that  $W_{\text{sample,M}}$  and  $W_{\text{sample,S}}$  have negligible domain-to-domain variation, a bimodal distribution of  $W_{\text{sample}}$  would be observed and the full width at half maximum (FWHM) of the distribution would be greatest at the intermediate temperature. However, such is contrary to this work's KPFM results: the FWHM of histograms of  $W_{\text{sample}}$  at three different temperatures ( $\sim 0.1$  eV) did not vary greatly [Fig. 2(c)].

Figures 3(a) shows schematic energy band diagrams of the metallic ( $M_{\text{VO}_2}$ ) and the semiconducting ( $S_{\text{VO}_2}$ ) VO<sub>2</sub> domains that coexist during the MIT. Local work function in the  $S_{\text{VO}_2}$  domains decreases, approaching the  $M_{\text{VO}_2}$ - $S_{\text{VO}_2}$  domain boundaries due to band bending [Fig. 3(b)]. If the  $S_{\text{VO}_2}$  domain size is comparable to the width of the space-charge-region (SCR), the local  $W_{\text{sample}}$  in those domains is smaller than  $W_{\text{sample,S}}$  [Fig. 3(c)] and Eq. (1) loses validity. Instead, the FWHM of  $W_{\text{sample}}$  may show little temperature dependence, as per the KPFM results of Fig. 2. Assuming a carrier density ( $N$ ) of  $10^{16}$ – $10^{18}$   $\text{cm}^{-3}$ , a relative dielectric ( $\epsilon$ ) of 30, and built-in potential ( $\phi_{bi}$ ) of 0.18 eV for VO<sub>2</sub> at 60 °C, the SCR width,  $\sqrt{\frac{2\epsilon}{qN}(\phi_{bi} - \frac{2kT}{q})}$ , would be 24–240 nm ( $q$ : electron charge,  $k$  the Boltzmann constant, and  $T$ : temperature).<sup>3</sup> If the  $S_{\text{VO}_2}$  domains are at least twice size of the SCR width, they would have regions not undergoing band bending. The  $W_{\text{sample,S}}$  maps observed here and other nanoscopic domain images<sup>6,10</sup> show  $S_{\text{VO}_2}$  domains as small as tens of nm. Therefore, band bending throughout the  $S_{\text{VO}_2}$  domains is possible in VO<sub>2</sub> thin films, leading to a reduction of  $W_{\text{sample}}$ .

To confirm the relationship between  $W_{\text{sample}}$  and resistivity, surface potential maps were recorded under an applied

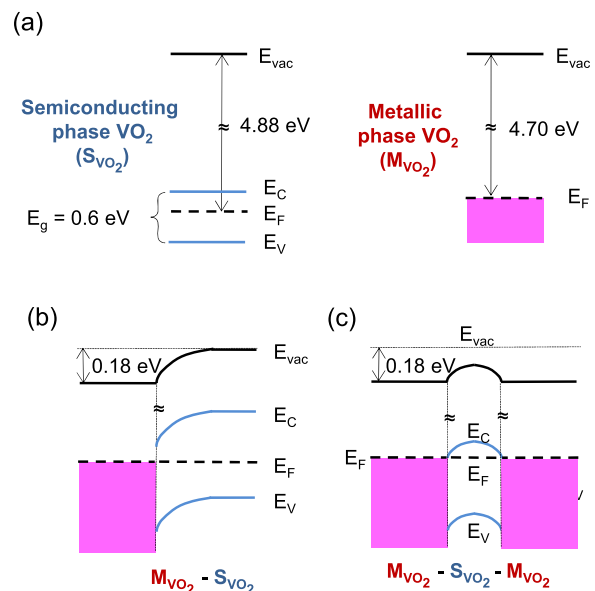


FIG. 3. Energy band diagrams of (a) metallic VO<sub>2</sub> ( $M_{\text{VO}_2}$ ) and semiconducting VO<sub>2</sub> ( $S_{\text{VO}_2}$ ), (b)  $M_{\text{VO}_2}$ - $S_{\text{VO}_2}$  interface with  $S_{\text{VO}_2}$  domains larger than the SCR width, and (c)  $M_{\text{VO}_2}$ - $S_{\text{VO}_2}$ - $M_{\text{VO}_2}$  region for  $S_{\text{VO}_2}$  domains smaller than the SCR width. Case (a) describes the band for a single, homogeneous phase. Cases (b) and (c) describe band bending in the vicinity of the domain boundaries of an electronically inhomogeneous sample near  $T_{\text{MIT}}$ .

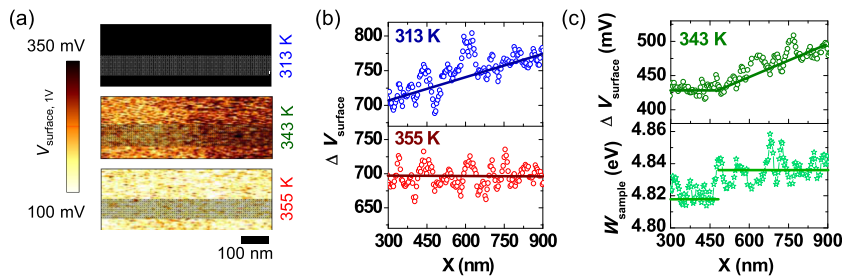


FIG. 4. (a) Maps of surface potential under an applied bias voltage of 1 V between the electrodes on the VO<sub>2</sub> ( $V_{\text{surface},1V}$ ). (b) profiles of  $\Delta V_{\text{surface}} = V_{\text{surface},1V} - V_{\text{surface},0V}$ , at 313 and 355 K, and (c) profiles of  $\Delta V_{\text{surface}}$  and  $W_{\text{sample}}$  at 343 K.

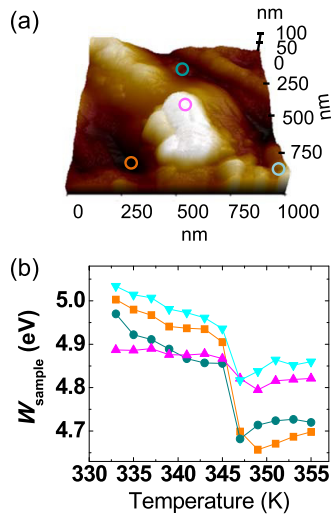


FIG. 5. (a) Topography and four selected regions (denoted as colored circles) of a VO<sub>2</sub> thin film surface and (b) temperature dependence of local  $W_{\text{sample}}$  taken at the four regions.

external bias voltage ( $V_{\text{ext}}$  in Fig. 1) of 1 V between the electrodes on the VO<sub>2</sub> sample [Fig. 4]. In the subscripts X, V denotes the applied potential:  $\Delta V_{\text{surface}}$  is defined as  $[V_{\text{surface},1V} - V_{\text{surface},0V}]$ , which corresponds to the local potential drop, free of any local variation of  $W_{\text{sample}}$ .  $\Delta V_{\text{surface}}$  profiles show clear temperature dependence. Greater slopes in the  $\Delta V_{\text{surface}}$  profiles were shown at lower temperature by the semiconducting state; they reduced at higher temperature with the emergence of the metallic state [Figs. 4(b) and 4(c)]. At the intermediate temperature, two distinct regions with different slopes were observed, indicating the coexistence of two electronic phases. Figure 4(c) also shows that the slope of the  $\Delta V_{\text{surface}}$  profiles varied with changing  $W_{\text{sample}}$ . These results demonstrate that KPFM allows observation of local resistivity and the accompanying electronic states of the VO<sub>2</sub> thin film.

Spatial variation of local  $W_{\text{sample}}$  was also examined: four locations were selected [colored circles in Fig. 5(a)].  $W_{\text{sample}}$ , averaged for each of 50 nm diameter circular areas decreased during heating [Fig. 5(b)]. Vanadium oxides can form several compounds, but only VO<sub>2</sub> phase exhibits a MIT near 340 K.<sup>6</sup> If the surface composition greatly deviated from VO<sub>2</sub> phase,  $W_{\text{sample}}$  would not change during the MIT. Therefore, the results in Fig. 5 indicate that the sample did not have a significantly off-stoichiometric surface composition. Yin *et al.* found that the surface of a VO<sub>2</sub> thin film underwent irreversible electronic changes during heating cycles in ultrahigh vacuum due to the removal of oxygen.<sup>7</sup>

KPFM, which does not require vacuum conditions, may avoid such unwanted reduction. The KPFM results here remained consistent during repeated measurement.

In summary, KPFM was used to observe the sharp drop of epitaxial VO<sub>2</sub> thin film's work function during its MIT, indicating changes in its electronic structure. The thin film's small domains were shown to undergo band bending adjacent to the domain boundaries, which altered the spatial distribution of carrier concentration and the resulting MIT behavior. Imaging domain distributions in VO<sub>2</sub> may aid the design of nanoscale devices that can utilize the large change of dielectric functions during the MIT as well as contribute to the understanding of the underlying phase transition mechanism.

This work was supported by the Quantum Metamaterials Research Center (2009-0063324), the Basic Research Program (2010-0009344), through the National Research Foundation of Korea Grant funded by the Korean Ministry of Education, Science, and Technology (MEST), and a Korea-CIS project of MEST in Korea, and MIT Creative Research Project in ETRI. C.K. and S.R. acknowledge AFOSR Grant No. FA9550-08-1-0203 for financial support.

- <sup>1</sup>T. M. Rice, H. Launois, and J. P. Pouget, *Phys. Rev. Lett.* **73**, 3042 (1994).
- <sup>2</sup>J. B. Goodenough, *J. Solid State Chem.* **3**, 490 (1971).
- <sup>3</sup>H.-T. Kim, B.-G. Chae, D.-H. Youn, S.-L. Maeng, G. Kim, K.-Y. Kang, and Y.-S. Lim, *New J. Phys.* **6**, 52 (2004).
- <sup>4</sup>B. S. Mun, K. Chen, J. Yoon, C. Dejoie, N. Tamura, M. Kunz, Z. Liu, M. E. Grass, S.-K. Mo, C. Park, Y. Y. Lee, and H. Ju, *Phys. Rev. B* **84**, 113109 (2011).
- <sup>5</sup>W.-T. Liu, J. Cao, W. Fan, Z. Hao, M. C. Martin, Y. R. Shen, J. Wu, and F. Wang, *Nano Lett.* **11**, 466 (2011).
- <sup>6</sup>Y. J. Chang, J. S. Yang, Y. S. Kim, D. H. Kim, T. W. Noh, D.-W. Kim, E. Oh, B. Kahng, and J.-S. Chung, *Phys. Rev. B* **76**, 075118 (2007).
- <sup>7</sup>W. Yin, S. Wolf, C. Ko, S. Ramanathan, and P. Reinke, *J. Appl. Phys.* **109**, 024311 (2011).
- <sup>8</sup>C. Ko, Z. Yang, and S. Ramanathan, *ACS Appl. Mater. Interfaces* **3**, 3396 (2011).
- <sup>9</sup>S. Zhang, I. S. Kim, and L. J. Lauhon, *Nano Lett.* **11**, 1443 (2011).
- <sup>10</sup>M. M. Qazilbash, A. Tripathi, A. A. Shafgans, B.-J. Kim, H.-T. Kim, Z. Cai, M. V. Holt, J. M. Maser, F. Keilmann, O. G. Shpyrko, and D. N. Basov, *Phys. Rev. B* **83**, 165108 (2011).
- <sup>11</sup>K. Appavoo and R. F. Haglund, Jr., *Nano Lett.* **11**, 1025 (2011).
- <sup>12</sup>T. Driscoll, H.-T. Kim, B.-G. Chae, B.-J. Kim, Y.-W. Lee, N. M. Jokerst, S. Palit, D. R. Smith, M. Di Ventra, and D. N. Basov, *Science* **325**, 1518 (2009).
- <sup>13</sup>H. Yin, M. Luo, K. Yu, Y. Gao, R. Huang, Z. Zhang, M. Zeng, C. Cao, and Z. Zhu, *ACS Appl. Mater. Interfaces* **3**, 2057 (2011).
- <sup>14</sup>R. Jaramillo and S. Ramanathan, *Adv. Funct. Mater.* **21**, 4068 (2011).
- <sup>15</sup>H. Kim, S. Hong, and D.-W. Kim, *Appl. Phys. Lett.* **100**, 022901 (2012).
- <sup>16</sup>V. E. Henrich and P. A. Cox, *The Surface Science of Metal Oxides* (Cambridge University Press, Cambridge, 1994).